

“Nanogranite” and glassy inclusions: The anatectic melt in migmatites and granulites

Bernardo Cesare¹, Silvio Ferrero¹, Emma Salvioli-Mariani², Danilo Pedron³, Andrea Cavallo⁴

¹Dipartimento di Geoscienze, Università di Padova, Via Giotto 1, 35137 Padua, Italy

²Dipartimento di Scienze della Terra, Università di Parma, Viale Usberti 157A, 43100 Parma, Italy

³Dipartimento di Scienze Chimiche, Università di Padova, Via Marzolo 1, 35131 Padua, Italy

⁴Istituto Nazionale di Geofisica e Vulcanologia, Via di Vigna Murata 605, 00143 Rome, Italy

ABSTRACT

Using as a case study a granulite from the Kerala Khondalite Belt, India, we show that a former anatectic melt can be preserved as tiny (<25 μm) droplets within refractory minerals, in this case garnet. The melt is either fully crystallized as a Qtz-Ab-Kfs-Bt cryptocrystalline aggregate (“nanogranite”), or completely glassy in inclusions <15 μm . Both nanogranite and glassy inclusions have a peraluminous, ultrapotassic granitic composition that, in this case, does not correspond to a “minimum melt” and points to high melting temperatures, in agreement with the ultrahigh-temperature origin of the rock. This discovery indicates that peritectic minerals, growing during incongruent melting reactions, act as hosts for inclusions of anatectic melt, and that in the general case of slow cooling of the crust these inclusions will occur as nanogranite. Exceptionally, in the smallest inclusions, glass may be present due to inhibition of crystallization. Our results extend the frontiers of petrological and geochemical research in crustal melting, as the composition of natural anatectic melts can be directly analyzed rather than assumed.

INTRODUCTION AND SAMPLE DESCRIPTION

Partial melting (anatexis) is the main agent of geochemical differentiation in Earth’s crust (Brown and Rushmer, 2006) and deeply affects lithosphere rheology and geodynamics (e.g., Vanderhaeghe, 2001). Crustal anatexis produces granitic melts (Clemens, 2006; Vielzeuf et al., 1990), whose segregation (Sawyer, 1996; Petford et al., 2000; Brown, 2007) results in the formation of granulites as the *residuum* of the melting process (Vielzeuf et al., 1990; Sawyer, 2008), and granitic leucosomes (Clemens, 1990; Sawyer and Brown,

2008) as relicts of incomplete melt extraction. An obstacle to the quantitative study of natural melting is that the composition of the melt is often unconstrained, because leucosome chemistry is generally affected by cumulus phenomena, fractional crystallization, or presence of xenocrysts (Sawyer, 1996, 2008; Marchildon and Brown, 2001). Therefore, melt composition is generally assumed from experimental studies (Sawyer, 2008). We tried to overcome such weakness with a novel small-scale approach to the geochemical characterization of anatectic melts, building on our recent research on glass inclusions in granu-

litic xenoliths from dacites in SE Spain (Acosta-Vigil et al., 2007, and references therein). There, we recognized that glass inclusions of leucogranitic composition were preserved by rapid cooling in several host minerals, in particular garnet, which had formed at $T > 800$ °C in the presence of melt. We interpreted these findings as results of incongruent reactions producing an anatectic melt that was trapped by the growing peritectic minerals (Cesare et al., 2009), and predicted that inclusions of anatectic melt should be present also in granulites and migmatites (Cesare, 2008). For the present study we selected samples from the world-famous granulites from the Proterozoic Kerala Khondalite Belt, India, as representatives of a regional anatectic crustal terrain (see the GSA Data Repository¹ [and Fig. DR1 within the Repository] for further geological and petrological information). These rocks underwent ultrahigh-temperature metamorphism and partial melting during the Pan-African orogeny, with the development of migmatites characterized by Qtz-feldspars leucosomes and Grt-Crd-Sil-Bt-bearing melanosomes (khondalites; Fig. DR2). Garnet mostly occurs in the latter, as centimeter-sized anhedral porphyroblasts, mantled by cordierite and wrapped by a foliation outlined by sillimanite and graphite (Fig. 1A). Garnet, which often includes crystals of biotite and sillimanite, in places contains also clusters of tiny (2–25 μm across) inclusions (Figs. 1B, 2, and DR3A). Clusters are <2 mm across, contain hundreds of inclusions, do not have a preferred microstructural location in the garnet host, but never touch garnet boundaries. These microstructural features indicate that inclusions are *primary*, i.e., trapped by garnet during its growth (Roedder, 1984). Inclusions are generally made of a polycrystalline aggregate of birefringent crystals (Figs. 1C and 1D), but in places they are monophasic (Figs. 2C and DR3A) and optically isotropic (hereafter referred to as “glassy”). Polycrystalline inclusions are slightly larger (5–25 μm ; Fig. 3A) than the glassy ones (2.5–17.5 μm ; Fig. 3B); in both cases they are subspherical, commonly faceted

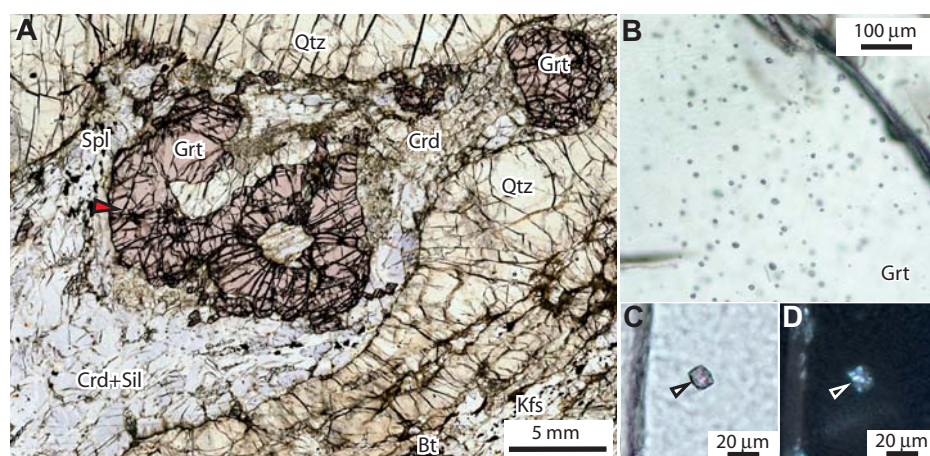


Figure 1. A: Melanosome of a khondalite, containing garnet (Grt), partly replaced by cordierite (Crd), in a foliated matrix with sillimanite (Sil) and quartz (Qtz). K-feldspar (Kfs), rare biotite (Bt), and spinel (Spl) also occur. Red arrow points to a cluster of melt inclusions. B: Cluster containing both nanogranite and glassy inclusions in garnet from A. C: Close-up of a nanogranite inclusion with negative crystal shape. D: Cross-polarized image of C, showing that inclusion consists of a birefringent polycrystalline aggregate.

¹GSA Data Repository item 2009146, supplementary methods, geological and petrographic information, and microchemical data (Tables DR1 and DR2, and Figures DR1–DR4), is available online at www.geosociety.org/pubs/ft2009.htm, or on request from editing@geosociety.org or Documents Secretary, GSA, P.O. Box 9140, Boulder, CO 80301, USA.

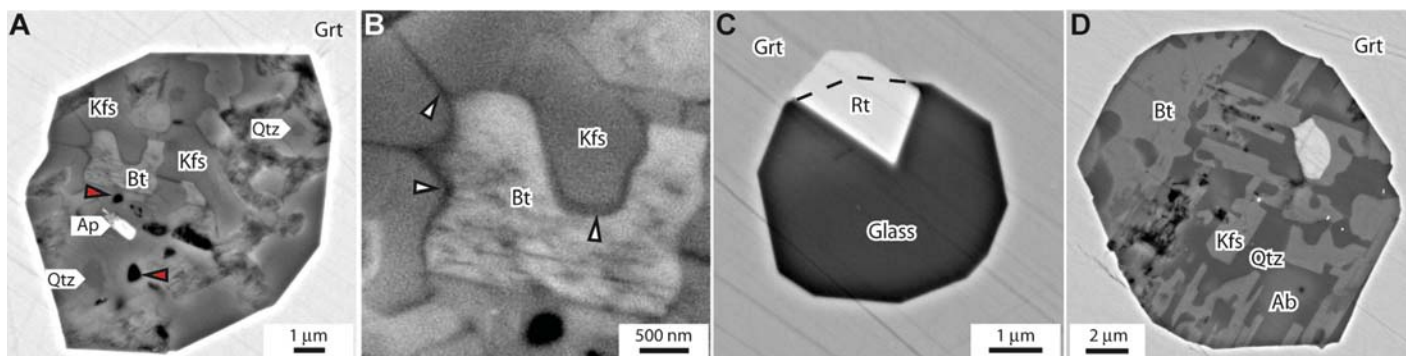


Figure 2. A: Backscattered electron (BSE) FESEM view of a nanogranite inclusion displaying a polycrystalline, micrometer-sized hypidiomorphic aggregate of Qtz, Kfs, Bt, and accessory apatite (Ap). Submicrometer empty cavities (red arrows) define an internal porosity. B: Close-up of A showing thin films (arrows) coating cusped-lobate boundaries between Bt and Kfs. The material constituting the films was not determined in this study. C: Glassy inclusion consisting of a homogeneous amorphous phase (glass) and one crystal of rutile (Rt). The shape of rutile and its relationships to the negative crystal inclusion walls (dashed line) indicate that rutile was already present at the time of melt entrapment. The lack of decrepitation microstructures and the absence of daughter minerals at inclusion walls (for comparison see Acosta-Vigil et al., 2007, their figure 3) suggest that the glass did not undergo postentrapment modifications (see also Fig. DR3B). D: Nanogranite inclusion with large, idiomorphic crystals of biotite and K-feldspar in a micrographic association with interstitial quartz and subordinate albite (Ab).

as negative crystals (Figs. 1C, 1D, 2A, and 2C). In places, inclusions may contain crystals, often zircon, apatite, or rutile (Figs. DR3B and DR3C), that were clearly already present at the time of entrapment (Fig. 2C), and probably favored the formation of the inclusion (see Roedder, 1984). The two typologies of inclusions are randomly distributed within clusters (Fig. DR3A), where glassy ones represent ~15% of the total. Given the extremely fine grain size of phases, at the limits of analytical resolution, inclusions have been characterized by a combination of electron microprobe (EMP), field emission scanning electron microscope (FESEM, in EDS, BSE, and X-ray

mapping modes), and micro-Raman techniques; in addition, polycrystalline inclusions were remelted in a high-*T* heating stage (for details on methods, see the GSA Data Repository).

“NANOGRANITE” INCLUSIONS

Polycrystalline inclusions consist of a multiphase aggregate with equigranular, hypidiomorphic to allotriomorphic texture, characterized by subhedral biotite and K-feldspar and anhedral quartz and plagioclase (Figs. 2A, 2D, and DR3C). Accessory minerals include apatite, rutile, titanite, zircon, and iron oxides. In places the texture tends to be inequigranular, or to contain granophyric to micrographic intergrowths of quartz and feldspars (Figs. 2D and DR3C). Owing to these features typical of intrusive magmatic rocks, and given the grain size of crystals in the range 10^{-2} – 10^1 μm , we have named these inclusions *nanogranite*. Nanogranite inclusions generally display a diffuse porosity with size of cavities down to a few tens of nanometers

of crystallizing melt. The 10–100-nm-thick films of unknown nature (quartz or glass) coating cusped-lobate phase boundaries (Fig. 2B) recall the pseudomorphing of melt-filled pores often seen at greater length scale in migmatites and granulites (Holness and Sawyer, 2008).

BSE imaging combined with X-ray mapping allows identification of the main phases and of the main textures in nanogranite inclusions. In the example of Figure 4 (see also Fig. DR4), one part of the inclusion has a coarse (>1 μm) grain size, whereas the other is much more fine-grained. From a chemical point of view, K seems to dominate over Na, and biotite appears to be richer in Mg than Fe, as confirmed by the EMP analyses that provide $X_{\text{Fe}} = 0.19$ – 0.25 (Table DR1).

The experimental remelting of the nanogranite inclusions brought about their homogenization but produced some interaction with the garnet host, with formation of peritectic phases and melt contamination by Fe and Mg. Despite such effect, and the unavoidable loss of sodium during EMP analysis with a focused beam, the

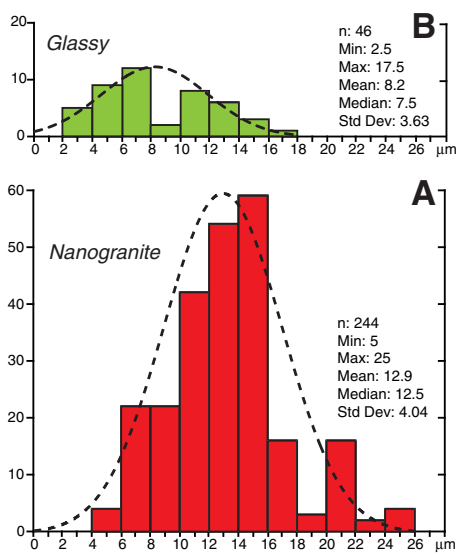


Figure 3. A: Histogram and Gaussian curve of the diameter (μm) of nanogranite inclusions measured in two clusters in one garnet. B: Histogram and Gaussian curve of the diameter of glassy inclusions in the same clusters.

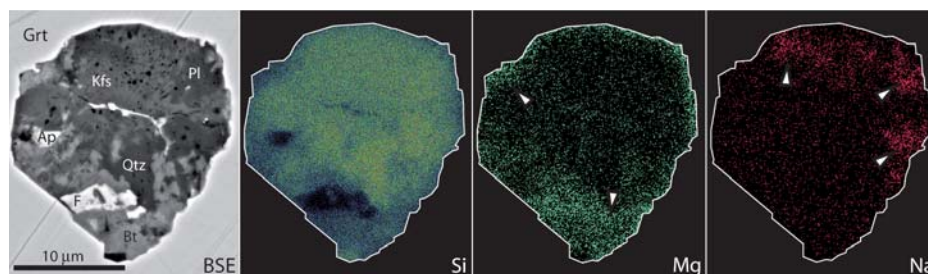


Figure 4. FESEM BSE image (left) and X-ray maps of Si, Na, and Mg for a nanogranite inclusion in garnet. Arrows on Na and Mg maps indicate areas of maximum element concentration in inclusions. The distribution of elements (see also Fig. DR4) allows identification of Qtz, Kfs, Bt, albitic Pl, Ap, and Fe-Mg oxide (F) in the BSE image.

composition of the remelted nanogranite is granitic and potassic, in agreement with the phase abundances observed with X-ray FESEM mapping. However, because of their contaminated composition, these analyses are not considered in the discussion and plots below.

GLASSY INCLUSIONS

Glassy inclusions contain an amorphous phase, as indicated by the micro-Raman spectrum (Fig. 5) that displays a prominent broad band centered at ~ 450 cm^{-1} , and less pronounced bands at ~ 590 , 790 , and 1140 cm^{-1} . These bands are characteristic of rhyolitic glasses, as shown by the spectrum of an anhydrous haplogranitic glass synthesized by Morgan and London (2005).

The noncrystalline nature of these inclusions is indirectly attested also by their composition, incompatible with any rock-forming silicate. EMP analyses of the glass (Table DR2) again indicate a persilic composition, very high in K_2O (>7 wt%) and low in Na_2O (<1 wt%) even after correction for Na loss; see the GSA Data Repository) and CaO, with 1–2 wt% FeO. Glasses have an ASI (aluminum saturation index) in the range 1.2–1.4, typical of granitic melts in equilibrium with peraluminous minerals (Acosta-Vigil et al., 2003), and 2–4 wt% normative corundum. On a normative Q-Ab-Or diagram (Fig. 6), glassy inclusions plot close to the Q-Or side, at $Q/(Q + \text{Or})$ in the range 0.42–0.51. This felsic, peraluminous, ultrapotassic rhyolitic composition is far from haplogranitic *minimum melts* (Johannes and Holtz, 1996). Although not common in nature, it is similar to that of lavas from the Malani Group (India), considered the products of high-temperature crustal anatexis (Maheshwari et al., 1996), and to that of experimental glasses obtained from the water-absent partial melting of Na-poor natural pelites (Patiño Douce and Johnston, 1991). The very low Na content of glassy inclusions is in agreement with the lack of plagioclase in the studied melanosome and suggests that the melting reaction was close to the (Ti)KFMASH end member $\text{Bt} + \text{Sil} + \text{Qtz} \pm \text{Ilm} = \text{melt} + \text{Grt} \pm \text{Rt}$ (Patiño Douce and Johnston, 1991). Even considering the uncertainty in Na contents (Morgan and London, 2005), EMP totals suggest very low $a_{\text{H}_2\text{O}}$ for the formation of melts in the glassy inclusions. This is consistent with the presence of carbonic fluid inclusions in the same rocks, without detectable aqueous phase (S. Ferrero, unpublished data), and is also supported by the low FeO content of glass, which is known to increase with increasing H_2O in the melt (Patiño Douce, 1996). Therefore, considering the maximum H_2O content (4 wt%; Table DR2), the glass compositional data indicate melts produced at temperatures ≥ 850 $^\circ\text{C}$, in agreement with petrological studies showing that garnet growth

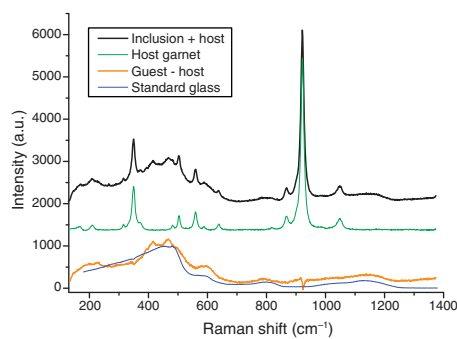


Figure 5. Stack of the micro-Raman spectra of a glassy inclusion in garnet from a Kerala Khondalite Belt khondalite (black), of the garnet host (green), and of the glassy inclusion after subtraction of the contribution of garnet (orange). The latter is comparable with the spectrum of synthetic anhydrous haplogranitic standard glass (blue) (Morgan and London, 2005). Intensities in arbitrary units.

by the dehydration melting of biotite took place in these rocks at 6–8 kbar and $T > 900$ $^\circ\text{C}$ (e.g., Nandakumar and Harley, 2000).

CAUSES OF GLASS PRESERVATION

The occurrence of glassy inclusions is another striking aspect of our research, because melt is normally expected to crystallize completely in regional, slowly cooled migmatite terrains. Since geochronological data indicate that, after anatexis, the rocks of the Kerala Khondalite Belt took at least 60 Ma to cool from 850 $^\circ\text{C}$ to ~ 350 $^\circ\text{C}$ (Cenki et al., 2004), the delay in nucleation by supercooling of melt in inclusions (Donaldson, 1979) should be minimal and negligible for the present discussion, and we can rule out very rapid cooling as the possible cause of glass preservation. Another cause could be the chemical composition of glass, for example a high viscosity or low volatile content slowing down diffusion of elements toward growing nuclei. As noted above, however, glassy inclusions coexist with totally crystallized ones in the same clusters (see Fig. DR3A), and it is unlikely that chemical inhomogeneities in granitic melts can occur at length scales <100 μm . One measurable parameter differing among glassy and nanogranite inclusions is size: The histograms of the diameter of inclusions reported in Figure 3 clearly show that glassy and nanogranite inclusions have different size distributions, with mean values at 8.2 and 12.9 μm , respectively. Although there is a significant overlap, the two populations are statistically different, and we propose that this difference in size was influential in the crystallization of melt droplets, so that (most of) the smaller inclusions remained amorphous (glassy) because of inhibited nucleation. The control of pore size on nucleation is a well-known phenomenon in

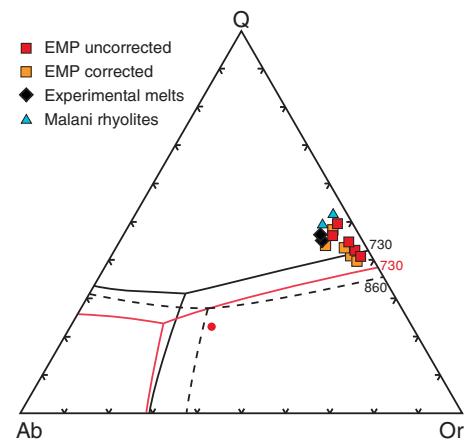


Figure 6. Composition of analyzed melts in the CIPW Q-Ab-Or diagram, comparing both uncorrected and corrected EMP analyses of glassy inclusions from Table DR2 with the experimental glass compositions of Patiño Douce and Johnston (1991) and the ultrapotassic rhyolites of the Malani Group (India; Maheshwari et al., 1996). Black lines—minima and cotectic curves for the subaluminous haplogranite system at 5 kbar, with $a_{\text{H}_2\text{O}} = 1$ (solid) and $a_{\text{H}_2\text{O}} = 0.5$ (dashed). Red lines—curves for the haplogranite system at 10 kbar with $a_{\text{H}_2\text{O}} = 1$. Red circle—minimum melt composition at 10 kbar, $a_{\text{H}_2\text{O}} = 0.5$. In the peraluminous system, cotectic curves move toward Q-richer compositions (Johannes and Holtz, 1996). Numbers refer to the temperature ($^\circ\text{C}$) of beginning of melting at the cotectic compositions on the Q-Or join.

aqueous solutions (Putnis et al., 1995), where the finer pores maintain a higher threshold supersaturation. However, the critical physicochemical parameters of this process are still obscure, especially in silicate melts from which it is also reported (Holness and Sawyer, 2008); aspects such as diffusion gradients in the confined fluid and/or the critical dimension of crystal nuclei are qualitatively important (Putnis et al., 1995; Muncill and Lasaga, 1988). In this respect, it is interesting to note that (1) reported critical nucleus dimensions are 100–500 nm for olivine, and (2) plagioclase has much slower nucleation kinetics possibly due to a considerably larger critical nucleus size (Donaldson, 1979; Muncill and Lasaga, 1988). Therefore, crystallization was probably inhibited because the small inclusion volume did not allow the establishment of concentration gradients high enough to form the “large” critical nuclei of feldspar.

CONCLUSIONS

Our results support the view that the studied inclusions are indeed witness to the melt that was trapped by peritectic garnet growing during the dehydration melting of biotite. Being trapped during a prograde event of magma formation, these granitic inclusions differ from

other occurrences such as those found in zircon from granitoid rocks (e.g., Thomas et al., 2002; Hopkins et al., 2008) that formed during magma crystallization upon cooling. Based on this perspective, and depending on *P-T-X* conditions, other peritectic phases such as orthopyroxene, spinel, cordierite, and ilmenite may be potential hosts to melt inclusions and should be carefully (re)investigated. Melt inclusions, so far studied in volcanic and shallow plutonic rocks (Sawyer, 2008) but found here for the first time in garnet from migmatites and granulites, widen the horizons in crustal petrology because, as we have shown, reliable petrological and geochemical information on anatexis can be gained from nanometer- to micrometer-scale objects. As an example, along with demonstrating that garnet growth was supersolidus, our results highlight the potential pitfalls of assuming anatectic melt as having a minimum melt composition, or of considering almost binary normative Q-Or compositions as “fractionated” (see for example Sawyer, 2008).

The possibility of entrapment of melt inclusions during anatexis depends on several parameters such as the amount of melt in the rock, the stress field acting on it, the growth rate of peritectic minerals, and the presence of impurities. The preservation of inclusions will essentially depend on the extent of chemical interaction with the host mineral, and on the mechanical behavior of the host during the subsequent history, as microfracturing would allow access of fluids and alteration of the primary melt composition or nanogranite assemblage. Therefore, melt inclusions should be targeted in strong minerals from the least deformed rock domains. Finally, our case study also highlights the possibility of finding “frozen” anatectic melt still preserved as glass, even in slowly cooled migmatites and granulites (see also Braga and Massonne, 2008), but we expect it to be restricted to inclusions <10–15 μm .

ACKNOWLEDGMENTS

We thank Antonio Acosta-Vigil, Bob Bodnar, Jamie Connolly, Satish Kumar, Lara Maritan, Dave Pattison, Manuel Rigo, and Lucie Tajcmanova for discussion, and Simon Harley, David London, and Alberto Patiño Douce for their reviews. This work was supported by Italian Ministry of Education, University, and Research grant PRIN 2007278A22 to Cesare.

REFERENCES CITED

Acosta-Vigil, A., London, D., Morgan, G.B., VI, and Dewers, T.A., 2003, Solubility of excess alumina in hydrous granitic melts in equilibrium with peraluminous minerals at 700–800 °C and 200 MPa, and applications of the aluminum saturation index: *Contributions to Mineralogy and Petrology*, v. 146, p. 100–119, doi: 10.1007/s00410-003-0486-6.

Acosta-Vigil, A., Cesare, B., London, D., and Morgan, G.B., VI, 2007, Microstructures and com-

position of melt inclusions in a crustal anatectic environment: The metapelitic enclaves within El Hoyazo dacites, SE Spain: *Chemical Geology*, v. 237, p. 450–465, doi: 10.1016/j.chemgeo.2006.07.014.

Braga, R., and Massonne, H.-J., 2008, Mineralogy of inclusions in zircon from high-pressure crustal rocks from the Ulten Zone, Italian Alps: *Periodico di Mineralogia*, v. 77, p. 43–64.

Brown, M., 2007, Crustal melting and melt extraction, ascent and emplacement in orogens: Mechanisms and consequences: *The Geological Society of London Journal*, v. 164, p. 709–730, doi: 10.1144/0016-76492006-171.

Brown, M., and Rushmer, T., 2006, Evolution and differentiation of the continental crust: Cambridge, UK, Cambridge University Press, 553 p.

Kenki, B., Braun, I., and Bröcker, M., 2004, Evolution of the continental crust in the Kerala Khondalite Belt, southernmost India: Evidence from Nd isotope mapping combined with U-Pb and Rb-Sr geochronology: *Precambrian Research*, v. 134, p. 275–292, doi: 10.1016/j.precamres.2004.06.002.

Cesare, B., 2008, Crustal melting: Working with enclaves, in Sawyer, E.W., and Brown, M., eds., *Working with migmatites: Quebec, Mineralogical Association of Canada, Short Course Series*, v. 38, p. 37–55.

Cesare, B., Rubatto, D., and Gómez-Pugnaire, M.T., 2009, Do extrusion ages reflect magma generation processes at depth? An example from SE Spain: *Contributions to Mineralogy and Petrology*, v. 157, p. 267–279, doi: 10.1007/s00410-008-0333-x.

Clemens, J.D., 1990, The granulite-granite connection, in Vielzeuf, D., and Vidal, P., eds., *Granulites and crustal differentiation: Dordrecht, Kluwer Academic Publishers*, p. 25–36.

Clemens, J.D., 2006, Melting of the continental crust: Fluid regimes, melting reactions, and source-rock fertility, in Brown, M., and Rushmer, T., eds., *Evolution and differentiation of the continental crust: Cambridge, UK, Cambridge University Press*, p. 296–331.

Donaldson, C.H., 1979, An experimental investigation of the delay in nucleation of olivine in mafic magmas: *Contributions to Mineralogy and Petrology*, v. 69, p. 21–32, doi: 10.1007/BF00375191.

Holness, M.B., and Sawyer, E.W., 2008, On the pseudomorphing of melt-filled pores during the crystallization of migmatites: *Journal of Petrology*, v. 49, p. 1343–1363, doi: 10.1093/petrology/egn028.

Hopkins, M., Harrison, M.T., and Manning, C.E., 2008, Low heat flow inferred from >4 Gyr zircons suggests Hadean plate boundary interactions: *Nature*, v. 456, p. 493–496, doi: 10.1038/nature07465.

Johannes, W., and Holtz, F., 1996, *Petrogenesis and experimental petrology of granitic rocks: Berlin, Springer*, 335 p.

Maheshwari, A., Coltorti, M., Sial, A.N., and Mariano, G., 1996, Crustal influences in the petrogenesis of the Malani rhyolite, southwestern Rajasthan: Combined trace element and oxygen isotope constraints: *Journal of the Geological Society of India*, v. 47, p. 611–619.

Marchildon, N., and Brown, M., 2001, Melt segregation in late syn-tectonic anatectic migmatites: An example from the Onawa contact aureole, Maine, USA: *Physics and Chemistry of the Earth, Part A: Solid Earth and Geod-*

esy, v. 26, p. 225–229, doi: 10.1016/S1464-1895(01)00049-7.

Morgan, G.B., VI, and London, D., 2005, Effect of current density on the electron microprobe analysis of alkali aluminosilicate glasses: *American Mineralogist*, v. 90, p. 1131–1138, doi: 10.2138/am.2005.1769.

Muncill, G.E., and Lasaga, A.C., 1988, Crystal-growth kinetics of plagioclase in igneous systems: Isothermal H₂O-saturated experiments and extension of a growth model to complex silicate melts: *American Mineralogist*, v. 73, p. 982–992.

Nandakumar, V., and Harley, S.L., 2000, A reappraisal of the pressure-temperature path of granulites from the Kerala Khondalite Belt, southern India: *Journal of Geology*, v. 108, p. 687–703, doi: 10.1086/317947.

Patiño Douce, A.E., 1996, Effects of pressure and H₂O content on the compositions of primary crustal melts: *Transactions of the Royal Society of Edinburgh, Earth Sciences*, v. 87, p. 11–21.

Patiño Douce, A.E., and Johnston, A.D., 1991, Phase equilibria and melt productivity in the pelitic system: Implications for the origin of peraluminous granitoids: *Contributions to Mineralogy and Petrology*, v. 107, p. 202–218, doi: 10.1007/BF00310707.

Petford, N., Cruden, A.R., McCaffrey, K.J.W., and Vigneresse, J.-L., 2000, Granite magma formation, transport and emplacement in the Earth's crust: *Nature*, v. 408, p. 669–673, doi: 10.1038/35047000.

Putnis, A., Prieto, M., and Fernandez-Diaz, L., 1995, Fluid supersaturation and crystallization in porous media: *Geological Magazine*, v. 132, p. 1–13.

Roedder, E., 1984, Fluid inclusions: *Mineralogical Society of America, Reviews in Mineralogy*, v. 12, 644 p.

Sawyer, E.W., 1996, Melt-segregation and magma flow in migmatites: Implications for the generation of granite magmas: *Transactions of the Royal Society of Edinburgh, Earth Sciences*, v. 87, p. 85–94.

Sawyer, E.W., 2008, Atlas of migmatites: *Quebec, Mineralogical Association of Canada, The Canadian Mineralogist Special Publication 9*, 386 p.

Sawyer, E.W., and Brown, M., 2008, Working with migmatites: *Quebec, Mineralogical Association of Canada, Short Course Series*, v. 38, 158 p.

Thomas, J.B., Bodnar, R.J., Shimizu, N., and Sinha, A.K., 2002, Determination of zircon/melt trace element partition coefficients from SIMS analysis of melt inclusions in zircon: *Geochimica et Cosmochimica Acta*, v. 66, p. 2887–2901, doi: 10.1016/S0016-7037(02)00881-5.

Vanderhaeghe, O., 2001, Melt segregation, pervasive melt migration and magma mobility in the continental crust: The structural record from pores to orogens: *Physics and Chemistry of the Earth, Part A: Solid Earth and Geodesy*, v. 26, p. 213–223, doi: 10.1016/S1464-1895(01)00048-5.

Vielzeuf, D., Clemens, J.C., Pin, C., and Moinet, E., 1990, Granites, granulites and crustal differentiation, in Vielzeuf, D., and Vidal, P., eds., *Granulites and crustal differentiation: Dordrecht, Kluwer Academic Publishers*, p. 59–85.

Manuscript received 19 December 2008

Revised manuscript received 23 February 2009

Manuscript accepted 28 February 2009

Printed in USA